ELSEVIER

Journal of Electroanalytical Chemistry 432 (1997) 205–214

JOURNAL OF ELECTROANALYTICAL CHEMISTRY

Origin of electrocatalysis in the reduction of peroxodisulfate on gold electrodes

Zdeněk Samec *, Alexander M. Bittner, Karl Doblhofer

Fritz-Haber-Institut der Max-Planck-Gesselschaft, Faradayweg 4-6, D-14 195 Berlin, Germany

Received 14 January 1997; revised 20 March 1997

Abstract

Stationary and rotating disc electrode voltammetry are employed to study the kinetics of the peroxodisulfate reduction to sulfate on Au(110) and Au(111) electrodes in the perchloric acid solution. The surface and the interfacial structure of these electrodes are examined by ex-situ STM and impedance measurements, respectively. Strong adsorption of peroxodisulfate and/or sulfate on both surfaces is observed, which has the superequivalent character, and which is controlled mainly by the charge on the metal. The surface structure and symmetry of the Au(111) surface allows for a more effective overlap of the electronic wave functions of the metal and the adsorbed peroxodisulfate, which results in a two order of magnitude faster electron transfer than on Au(110). On negatively charged surfaces, the rate of this electrocatalytic pathway is limited by the decreasing surface concentration of peroxodisulfate, while the rate of the electron transfer to the solution species (the direct pathway) can be measured. Its correction for the double layer effect reveals that the true kinetic parameters of the direct pathway have essentially the same values for both electrodes. A comparison of the kinetic behaviour of the flame-annealed and non-annealed Au(111) electrodes throws some light on the role of the steps on the metal surface. © 1997 Elsevier Science S.A.

1. Introduction

The effects of the nature of the electrode on electrode reactions have been broadly divided into two groups [1]. The primary effect may originate from the direct influence exerted by the electrode on the state of the reactant or the intermediate of an electrode reaction, comprising the case that the electrode itself is a reactant. On the other hand, the secondary effect occurs when the electrode affects the state of other species present, which themselves do not participate in the electrode reaction, but which may influence its rate. The most important of the primary and the secondary effects are the correlation of the rate of the electrode reaction with the adsorption energy of the reactant or the intermediate, and the modification of the electrical double layer, respectively.

Recently, both the primary and the secondary effects have been shown to play a significant role in the reduction of peroxodisulfate on gold electrodes [2,3]. On a polycrystalline gold [2] and single-crystal Au(111) [3] electrode, two following parallel pathways can be distinguished,

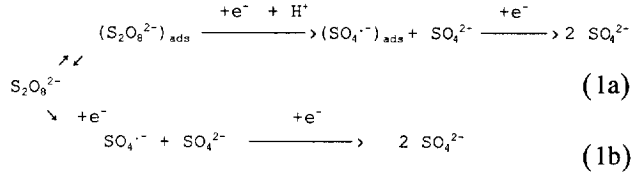

(1a)

(1b)

The electrocatalytic pathway (1a), which involves the adsorption of $S_2O_8^{2-}$ at the positively charged electrode surface and the reduction of the adsorbed anion with the intervening or following O–O bond breakage, prevails at the potentials more positive than the potential of zero charge. A considerably higher rate of this pathway at Au(111) has been ascribed to an increased adsorption and/or the increased rate of the electron transfer to adsorbed species due to a better matching of the anion structure with the trigonal symmetry of the Au(111) surface [3]. The direct pathway (1b) comprises the electron transfer to the peroxodisulfate anion in the solution. While the rate of this route is approximately the same at both Au(poly) and Au(111), it depends strongly on the factors

* Corresponding author. Permanent address: J. Heyrovský Institute of Physical Chemistry, Dolejškova 3, 182 23 Prague 8, Czech Republic. Fax: +42 2 8582307.

PII S0022-0728(97)00204-0

that influence the ion distribution on the solution side of the interface, such as the excess charge on the metal or the specific ion adsorption. A similar effect has been observed earlier on the mercury electrode [4].

The main aim of this work was to clarify the origin of electrocatalysis in the reduction of peroxodisulfate. In particular, we were interested in whether the catalytic effect arises from the differences in the peroxodisulfate adsorption and/or from the differences in the rate of the electron transfer to the adsorbed species. Therefore, we attempted to evaluate the contributions of these two factors to the reduction of the peroxodisulfate anion at the Au(111) and Au(110) electrodes, the surfaces of which exhibit the different structure and symmetry. In contrast to previous measurements [2,3], both Au(110) and Au(111) electrodes were pretreated by flame annealing. A comparison of the behaviour of Au(111) electrodes prepared in different ways was supposed to provide some additional information about the role of the electrode material.

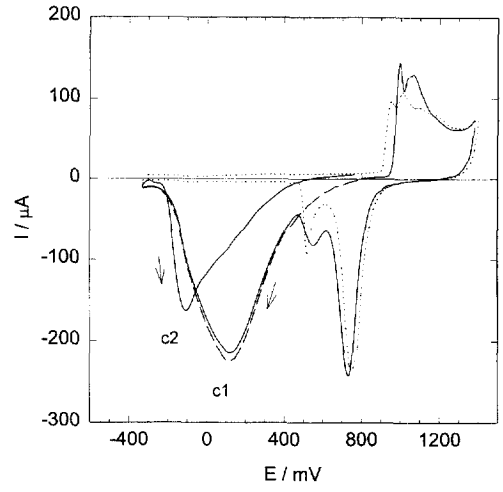

Fig. 1. Cyclic voltammogram of the stationary Au(110) electrode in 10 mM $HClO_4$ (· · ·), and in 10 mM $HClO_4$ + 1 mM $Na_2S_2O_8$ with the sweep starting at 0.8 V towards more positive (————) or more negative (- - -) potentials, at a sweep rate of 100 mV s^{-1}.

2. Experimental

Electrochemical measurements were carried out with single-crystal Au(110) and Au(111) electrodes, which were purchased from MaTecK (Jülich, Germany). The electrodes were prepared from 5N gold by the Czochralski method, oriented (< 1°), polished (< 0.03 μm) and cut in the form of a disc 1 mm thick and 9 mm in diameter (geometric area of 0.74 cm^2). The disc was cleaned in a mixture of sulfuric and nitric acid (1:1), rinsed with and stored in triply-distilled water. Prior to each experiment, the surface of the electrode was flame-annealed in the butane/air flame until it showed a dark red glow for 2 s, cooled for 30 s in air, and then quenched in the triply distilled water. All other experimental conditions, instrumentation and procedures have been described previously [3]. Electrode potentials are referred to the saturated calomel electrode (SCE).

3. Results

3.1. Cyclic and rotating disc electrode voltammetry of peroxodisulfate

Fig. 1 shows the cyclic voltammogram of the Au(110) electrode in the absence and in the presence of the peroxodisulfate anion in the 10 mM $HClO_4$ solution. As on the non-annealed Au(111) [3], the anion reduction can be seen at potentials more negative than approximately 0.8 V giving rise to the cathodic peak c1 and a shoulder c2. At far negative potentials, a drop in the reduction rate and, on the reversed sweep, an enhancement of the peak c2, are observed. Analogously, there seems to be no difference in the reduction rate on the gold surface, which is free of the surface oxides and polarized straight from 0.8 V towards more negative potentials (the dashed line in Fig. 1), and on the surface, which is oxidized first in a potential sweep from 0.8 V to 1.4 V (the full line in Fig. 1). Besides, the rate of the reduction of surface oxides is approximately the same as in the absence of peroxodisulfate, i.e. the two reduction processes appear to be additive. In order to minimize the possible interference with the surface oxidation and/or reduction, all polarization measurements were performed starting at 0.8 V towards more negative potentials on the electrodes previously polarized by a single sweep excursion from 0.8 V to −0.4 V and the reverse.

However, there is a considerable difference between the positions of the peak c1 at the Au(110) and Au(111) electrodes. This difference is apparent from Fig. 2, which shows the effects of the concentrations of peroxodisulfate (c^0) and the base electrolyte (c_B^0) on the peak potential E_p. On both the flame-annealed and the non-annealed Au(111) electrodes, the peak c1 appears at the potential which is more positive by about 300 mV than for Au(110). The effects of the sweep rate v and the concentrations c^0 and c_B^0 are otherwise very similar for all three gold electrodes. The height of the reduction peak c1 at the stationary electrode was found to be proportional to the square root of the sweep rate (v = 10 to 100 mV s^{-1}) and to the peroxodisulfate concentration (c^0 = 0.2 to 1.2 mM), while it was independent of the concentration of $HClO_4$ (c_B^0 = 10 to 1000 mM). On the other hand, the peak potential E_p varied with both the sweep rate v, $\partial E_p/\partial \log v = -57$ mV (10 mM $HClO_4$), the concentration c^0, $\partial E_p/\partial \log c^0 \approx -120$ mV, and the concentration c_B^0, $\partial E_p/\partial \log c_B^0 \approx 90$ mV.

The voltammograms of the rotating Au(110) and Au(111) electrodes are shown in Fig. 3. As in the previous study [3], the apparent rate constant k of the peroxodisul-

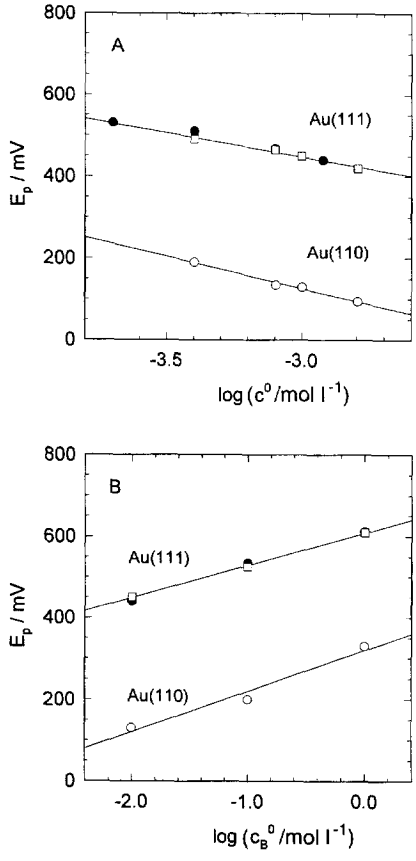

Fig. 2. Peak potential E_p vs. the logarithm of the concentration c^0 of peroxodisulfate in 10 mM $HClO_4$ (A) or the concentration c_B^0 of $HClO_4$ with 1 mM $Na_2S_2O_8$ (B) for the flame-annealed Au(110) and Au(111) (empty points) and the non-annealed Au(111) (full points). Sweep rate of 100 mV s^{-1}.

fate reduction was evaluated from the steady-state current I measured on a rotating disc electrode at a very low sweep rate (2 mV s^{-1}). Since the reduction proceeds with a high cathodic overpotential relative to the standard potential of the overall two-electron reaction $E^0 = 2.01$ V (vs. SHE), the backward reaction can be neglected and the rate constant expressed by the equation [5]

$$k = I/nFAc = \left[I_l/(I_l - I)\right](I/nFAc^0) \qquad (2)$$

where n is the number of electrodes consumed in the reaction, A is the electrode area and c is the peroxodisulfate concentration at the electrode, $I_l = 0.620\ n\ F\ A\ \nu^{-1/6}\ D^{2/3}\ \omega^{1/2}\ c^0$ is the limiting diffusion current (Levich's equation), ν is the kinematic viscosity, D is the diffusion coefficient and ω is the angular rotation speed. The applicability of Eq. (2) was checked by plotting $1/I$ vs. $\omega^{-1/2}$ (Koutecky–Levich plot) at various electrode potentials. These plots were linear with a slope corresponding to $D = (0.8 - 1.1) \times 10^{-5}$ cm^2 s^{-1} ($n = 2$), in good agreement with the literature data [2,6].

The main features of the kinetic behaviour of the flame-annealed Au(110) and Au(111) electrodes are apparent from Fig. 4. As indicated also by the voltammetric

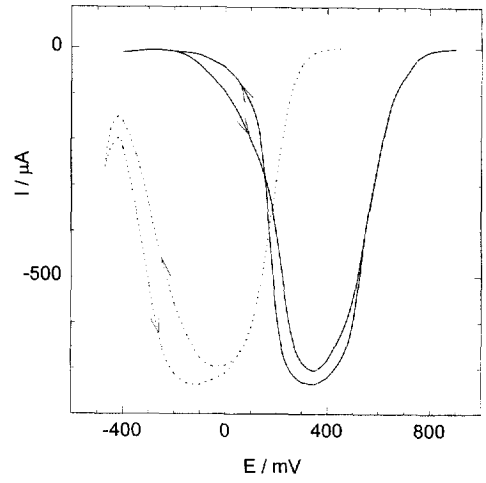

Fig. 3. Cyclic voltammograms of the rotating Au(111) (————) and Au(110) (· · ·) electrodes in 0.1 M $HClO_4$ + 1 mM $Na_2S_2O_8$ at the rotation velocity of 1040 rpm and the sweep rate of 2 mV s^{-1}. Both electrodes were flame-annealed prior to the measurement.

behaviour (Fig. 1 and Fig. 3), the dependence of the rate constant k on the electrode potential E has the shape of a *volcano* curve, which for the Au(111) electrode has the maximum at the potential that is about 350 mV more positive than for the Au(110) electrode. At far negative potentials, the rate constant increases with the increasing concentration of the base electrolyte on both electrodes. At far positive potentials, a similar effect is seen on Au(111), while on Au(110) the rate constant first decreases and then increases. An increase in the rate constant is apparently responsible for the change in the voltammetric peak potential E_p with c_B^0, which is about the same for both Au(111) and Au(110), cf. the slope $\partial E_p/\partial \log c_B^0 \approx 90$ mV in Fig. 2B. On the other hand, in the presence of sulfate, which adsorbs specifically at $E > 0.4$ V [7], the reduction rate on

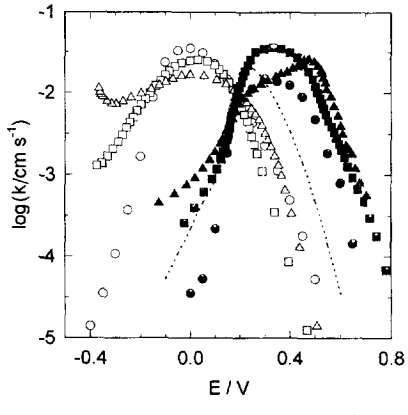

Fig. 4. Rate constant k of the peroxodisulfate reduction at the flame-annealed Au(110) (empty points) and Au(111) (full points and dotted line) electrodes in the solution containing 1 mM $Na_2S_2O_8$ and 0.01 M (●,○), 0.1 M (■,□) or 1M (▲,△) M $HClO_4$ or 0.01 M H_2SO_4 (· · ·) evaluated from the RDE voltammograms measured at the rotation velocity of 1040 rpm and the sweep rate of 2 mV s^{-1} going towards more negative potentials.

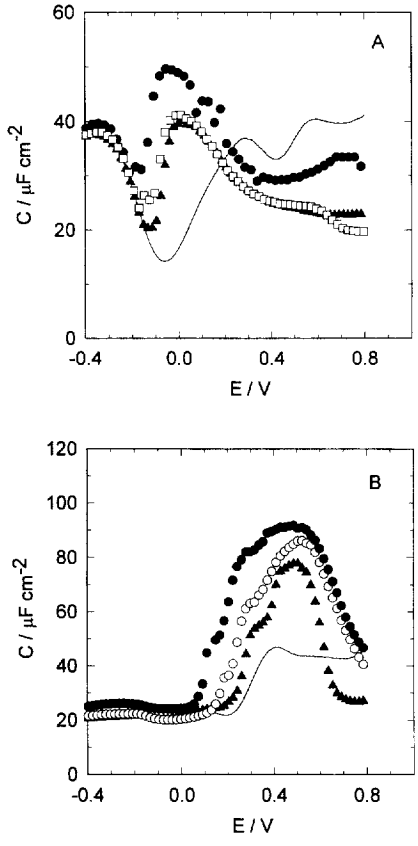

Fig. 5. Differential capacity C vs. the potential E for the Au(110) (A) and Au(111) (B) electrodes in 10 mM $HClO_4$ in the absence (full lines) and the presence (points) of peroxodisulfate at a concentration of 0.4 (▲), 0.8 (□), 1.0 (○) and 1.6 (●) mmol dm^{-3} measured at the rotation velocity of 1040 rpm and the sweep rate of 5 mV s^{-1} on going towards more positive potentials.

Au(111) drops by about one order of magnitude at far positive potentials, cf. the dotted line in Fig. 4.

3.2. The capacity of the Au(110) and Au(111) electrodes in the presence of peroxodisulfate

The complex impedance of the Au(110) and Au(111) electrodes was measured as a function of the potential by applying a 5 mV peak-to-peak perturbation a.c. signal at several frequencies (40, 70, 90, 200 Hz), the sweep rate of 5 mV s^{-1} and the rotation velocity 0 or 1060 rpm. The interfacial capacity was then evaluated for the equivalent circuit consisting of a resistor and a capacitor in series. While the resistance was the same in the presence and in the absence of peroxodisulfate, and its dependence on the potential did not exhibit any feature, the capacity of both electrodes changed considerably, cf. Fig. 5A and B. Neither the resistance, nor the capacity, were influenced by the a.c. frequency and the rotation velocity, which points to a negligible contribution of the parallel faradaic process to the measured impedance.

The absence of the effect of the faradaic process is supported by considerations based on the theory of the faradaic impedance in the case of an irreversible reaction [8]. An estimate based on this theory indicates that an a.c. faradaic peak should appear at about the same potential as the d.c. faradaic peak observed on either Au(110) or Au(111) electrode, cf. Fig. 3. However, the faradaic impedance is inversely proportional to the apparent charge transfer coefficient [8], which in this potential range is close to zero, cf. Fig. 4, i.e. the impedance should be very high. Outside this potential range, the apparent charge transfer coefficient approaches the value of ± 0.5, but the faradaic impedance rises again due to the decreasing rate constant.

There are two reasons why this conclusion is important. Firstly, owing to a coupling between the rates of the specific ion adsorption and the faradaic reaction, the fitting of impedance data to a particular equivalent circuit may not be straightforward, unless the contribution of one of these processes can be neglected [9]. Secondly, if the contribution of the faradaic impedance is negligible, the data can be fitted to the simple equivalent circuit above.

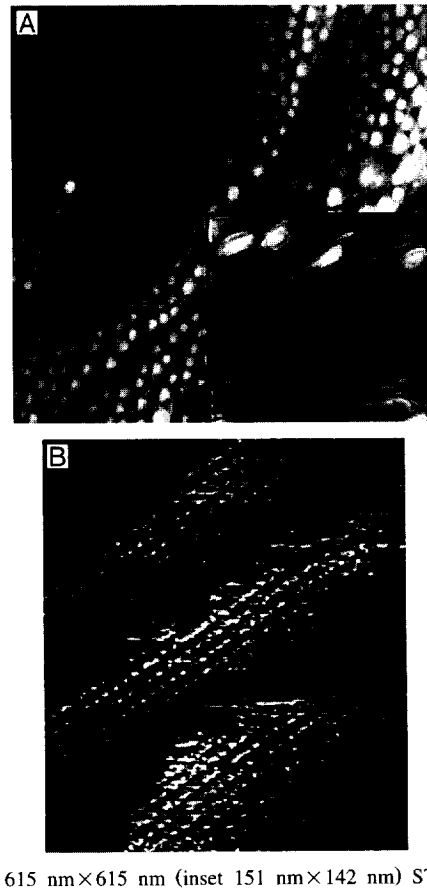

Fig. 6. A 615 nm×615 nm (inset 151 nm×142 nm) STM image of Au(111) (A) and a 11.3 nm×12.9 nm STM image of Au(110) (B) in air after flame-annealing, cycling in $HClO_4$ and rinsing with water. The surface of Au(111) is covered with holes and multilayer islands (clusters), which are separated by densely spaced steps. All holes and islands comprise terraces as seen in the inset. Four narrow terraces on Au(110) with a (1×1)-structure are shown (slightly distorted due to thermal drift).

3.3. STM of Au(110) and Au(111) electrodes

In order to establish a link between the surface structure of the Au(110) and Au(111) electrodes and their adsorption and kinetic behaviour, the ex situ STM images were obtained with the home-built STM [10] for the electrodes in air after their pretreatment by flame-annealing and cyclic polarization in 10 mM $HClO_4$ between −0.35 V and 1.35 V (ca. 50 cycles), and after their rinsing with triply distilled water. Such a pretreatment corresponds to the conditions met in the course of the voltammetric or impedance measurements of the peroxodisulfate reduction, involving the repeated excursions into the potential regions of the surface oxide formation and reduction. The typical images are displayed in Fig. 6.

4. Discussion

4.1. Surface structure of Au(111) and Au(110) electrodes

Both single-crystals exhibited faces which are flat, i.e. only very few nm high over lateral distances of several hundreds nm. The large scale structures of freshly annealed Au(111) and Au(110) without the intervening cycling are comparable with the literature data [11,12], though the surfaces were not perfect, namely the step density was quite high and, in the case of Au(111), we found many screw dislocations.

After the annealing and the cycling, the surface of Au(111) exhibited an unusual step-terrace topography, cf. Fig. 6A, which differed much from that of Au(110). Large parts of the surface were covered by holes and islands (three to five layers deep or high), which are completely terraced, i.e. the surface is still single crystalline. This structure is interrupted only by the areas with a high step density and the narrow terraces. We detected a similar structure without annealing and after the cycling of the Au(111) electrode in the previous work [3], though the step density was approximately twice as high. The narrow terraces showed an atomic (1×1) structure, i.e. the surface is unreconstructed. This is an expected result, because the 'herring bone' reconstruction is lifted at positive potentials during the cycling [12,13]. The step-terrace structure results probably from the well-known place exchange between Au and adsorbed O(H) at very positive potentials. Obviously, the potential-induced transport of Au atoms had occurred over several tens of nm leaving holes and forming islands. After using a less severe treatment consisting of a few potential sweeps under otherwise similar conditions, one finds holes and islands of mainly monoatomic depth or height [14,15]. The islands apparently comprise the missing atoms of the holes. It is interesting that the densely spaced narrow terraces (cf. the inset of Fig. 6A) are not covered by holes and islands. The multi-layered islands seem to have not enough space to be formed here. Instead, the Au ad-atoms on a narrow terrace are trapped by a step and, thereby contribute to the formation of a multi-layered island located next to such a step. In this way, a complete narrow terrace can be consumed.

A similar topography of the annealed Au(110) surface was observed irrespective of whether the Au(110) electrode was pretreated by cyclic polarization or not. Only small terraces were found, i.e. the density of steps is comparable to Au(111). Again, atomic resolution was achieved, as shown in Fig. 6B. Obviously, the (1×1) structure is present, while the usual (1×2) reconstruction is certainly lifted during cycling [11].

Owing to the comparable density of steps on Au(111) and Au(110) surfaces, the differences between the adsorption or kinetic behaviour of Au(111) and Au(110) electrodes should arise from different microscopic structural elements, not from the mesoscopic roughness. Indeed, the vast majority of the surface Au atoms is not located in steps, but on the terraces.

4.2. Adsorption of peroxodisulfate on Au(110) and Au(111) surfaces

An increase in the capacity of the Au(110) and Au(111) electrodes with the increasing concentration of peroxodisulfate in the solution (cf. Fig. 5) is probably caused by the specific adsorption of this anion or its reduction product (i.e. sulfate) on the metal surface. Since both anions apparently desorb from the surface at far negative potentials, an integration of the capacity starting at a sufficiently negative potential can yield the surface charge density σ on the metal, which should be related to the surface concentration of the adsorbed anions. Recently, chronocoulometric measurements of the surface charge on Au(111) in perchloric acid solutions containing sulfate have been used to determine the thermodynamic surface excess concentration of sulfate [7]. However, the application of a similar procedure to the adsorption of peroxodisulfate is considerably complicated by the intervening reduction of peroxodisulfate to sulfate. Obviously, the actual surface concentrations of peroxodisulfate and sulfate, Γ and Γ', respectively, depend on the rates of the adsorption, desorption and reduction processes. Besides, the rate of the adsorption of both anions is a function of their concentrations at the electrode, c and c', respectively, which can be affected by the rates of their transport in the solution. For example, at a rotating disc electrode, the steady-state concentrations c and c' can be related to the current I of the peroxodisulfate reduction by $c = (1 - I/I_l)c^0$ and $c' = (2\ I/I_l)c^0$, which reflect the overall 1:2 stoichiometry in the electrode reaction.

The surface concentrations Γ and Γ' could be inferred from the experimental capacity C on condition that the equilibrium is established in the adsorption of both anions, and that the anion adsorption exactly balances the changes in the anion concentrations at the electrode due to the

peroxodisulfate reduction, i.e. the equality $\Gamma'/c' = \Gamma/2c$ holds. Then, at a constant concentration of the base electrolyte, the electrocapillary equation can be written as

$$-\mathrm{d}\gamma = \sigma dE + \Gamma \mathrm{d}\mu + \Gamma' \mathrm{d}\mu' \quad (3)$$

Owing to the condition $\Gamma'/c' = \Gamma/2c$ and the relationship $c + (c'/2) = c^0$, which the anion concentrations at the electrode must fulfil, the term $\Gamma\ \mathrm{d}\mu + \Gamma' \mathrm{d}\mu'$ in Eq. (3) can be replaced by $RT(\Gamma + \Gamma')\mathrm{d}\ \ln c^0$, because $\Gamma \mathrm{d}\mu + \Gamma' \mathrm{d}\mu' = RT(\Gamma \mathrm{d}c/c + \Gamma' \mathrm{d}c'/c') = RT(\Gamma/c)\ \mathrm{d}c^0$ and $\Gamma + \Gamma' = \Gamma(c^0/c)$. Hence, the total surface excess $\Gamma_a = \Gamma + \Gamma'$ can be evaluated from

$$\Gamma_a = -(1/RT)(\partial\gamma/\partial \ln c^0) \quad (4)$$

An analysis of the kinetic model described in Section 4.4 indicates that the equilibrium in the adsorption of peroxodisulfate and sulfate could establish at sufficiently positive potentials, when the rate of the reduction of the adsorbed peroxodisulfate is low enough compared to the rate of the anion desorption. In order to examine whether the stoichiometric assumption leading to Eq. (4) is also realistic, the relative changes of the surface tension $\Delta\gamma$ were inferred by a double integration of the capacity C shown in Fig. 5. First, the capacity curves were integrated starting at the potential of -0.4 V. The surface charge σ at this potential was determined by the integration of the capacity curves in the absence of peroxodisulfate, which started at the potential of zero charge $E_{pzc} = -0.06$ V or 0.22 V at Au(110) or Au(111), respectively. The latter values represent the potentials, at which the capacity C is at a minimum, cf. the solid lines in Fig. 5A and B. The results of the second integration and the following differentiation according to Eq. (4) are displayed in Fig. 7A. The adsorption data for Au(111) can be compared with those reported for sulfate, which were determined from the chronocoulometric and radiochemical measurements at about the same anion concentration in the solution [7], cf. the triangles in Fig. 7A. Although the surface concentrations of both anions coincide, one should note that the adsorption of sulfate was measured in 0.1 M $HClO_4$ [7], and the data corresponds to a different charge σ on the metal. In fact, the comparison should be made at a constant value of σ [16]. Fig. 7B shows that the quantity Γ_a defined by Eq. (4) is then about twice as high as the thermodynamic (Gibbs) excess of sulfate. Hence, it can approximately represent the sum of the surface concentrations of sulfate and peroxodisulfate, to which sulfate contributes most when the faradaic current reaches a maximum, i.e. near the potential of zero charge ($\sigma = 0$), while at positive charges the contribution of peroxodisulfate prevails.

The data displayed in Fig. 7A suggest that the difference between the anion adsorption on Au(111) and Au(110) corresponds to the difference in the value of E_{pzc} for these two electrodes. Indeed, the difference between Au(111) and Au(110) appears to be rather small, when the surface

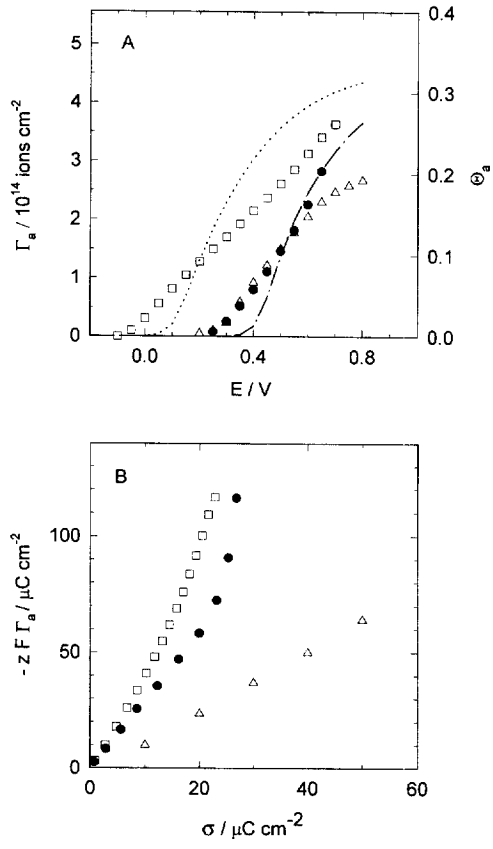

Fig. 7. Surface excess concentration Γ_a of peroxodisulfate vs. the potential E (A) and vs. the surface charge density on the metal σ (B) for Au(110) (□) and Au(111) (●) in 0.01 M $HClO_4$ + 0.4 mM $Na_2S_2O_8$. Adsorption data for Au(111) in 0.1 M $HClO_4$ + 0.5 mM K_2SO_4 (△) were taken from Ref. [7]. Simulated plots for Au(110) (· · ·) and Au(111) (– · –) represent the sum $\Gamma_a = \Gamma + \Gamma'$ evaluated by using Eq. (8) for the values of the parameters given in Table 1, and the common values of the parameters $\alpha_C = \gamma'' = 0.5$, $\gamma + \gamma' = 0.36$, $\beta = 0.64$ and assuming that Γ_a reaches the maximum corresponding to one-third of the atom density on the Au surface (1.39×10^{15} atoms cm^{-2}). θ_a in panel A relates the surface concentration to the atom density.

charge due to adsorbed anions, $z\ F\ \Gamma_a$ ($z = -2$), is correlated with the surface charge density σ, cf. Fig. 7B. Hence, the key factor in the anion adsorption appears to be the surface charge, and not the surface structure. Such a conclusion is corroborated by the observed strong adsorption of sulfate (bisulfate) on surfaces of sp-metals [17] or d-metals [18] exhibiting various structure and symmetry. However, the surface structure controls the position of the p.z.c. and, hence, it can exert an indirect influence on the ion adsorption.

At both Au(111) and Au(110), the estimated surface charge due to adsorbed anions is higher than the charge on the metal and, as in the case of sulfate [7], the adsorption exhibits the superequivalent character. This can have serious consequences for both the potential distribution in the electrical double layer and the adsorption of the counter ions (here mainly protons), which can be attracted to the

space charge region, so as to compensate for the superequivalent anionic charge [19].

4.3. Effect of the surface structure on the kinetics of the peroxodisulfate reduction

The kinetic behaviour of Au(poly), non-annealed Au(111) and flame-annealed Au(111) or Au(110) electrodes is compared in Fig. 8.

At $E > E_{pzc}$, the surface of all gold single-crystal electrodes should be covered by the adsorbed peroxodisulfate and/or sulfate. On the other hand, the concentration of peroxodisulfate in the space-charge region is probably very low owing to the electrical potential inversion, which is caused by the superequivalent anionic adsorption. Therefore, in this potential range, the contribution of the direct electron transfer then becomes quite negligible and the electrocatalytic pathway dominates. Hence, the reduction peak c1 on the cyclic voltammogram (Fig. 1) or the current maximum on the RDE voltammogram (Fig. 3), which occur always at a potential slightly more positive than E_{pzc}, can be associated with this pathway. The current maximum can arise from two concurrent factors. As the potential E decreases, the rate of the electron transfer to the adsorbed peroxodisulfate increases, while the surface concentration of peroxodisulfate decreases (Fig. 7A). A comparison of the rate constants at a sufficiently positive potential shows that the electrocatalytic pathway proceeds on Au(111) with the rate that is more than two orders of magnitude higher than on Au(110), cf. Fig. 4. On Au(poly), this pathway is even slower, giving rise only to a small shoulder at about 0.4 V [2], cf. the dotted line in Fig. 8. Since at far positive potentials the surface concentrations of peroxodisulfate on both Au(111) and Au(110) tend to reach about the same limit (Fig. 7A), the electrocatalytic effect is mainly due to a difference in the rate of the electron transfer between the metal and the adsorbate. The very fact that this rate is much higher for Au(111) points to a more effective overlap of the electronic wave functions of this surface and the reactant.

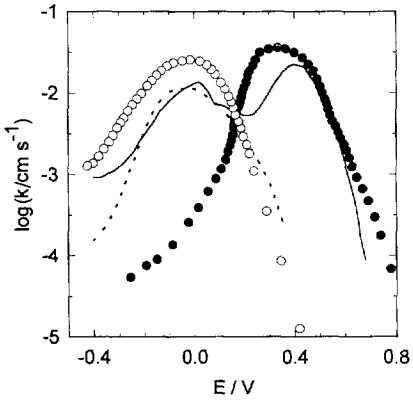

Fig. 8. Rate constant k of the peroxodisulfate reduction on the flame-annealed Au(110) (○), Au(111) (●), non-annealed Au(111)[3] (————) and Au(poly) [2] (· · ·) electrodes in 0.1 M $HClO_4$ + 1 mM $Na_2S_2O_8$ evaluated from the RDE voltammograms.

At far negative potentials, the reduction rate is considerably influenced by the electrostatic repulsion of the anion from the electrode surface [2–4]. On the negatively charged Au(poly) [2] and non-annealed Au(111) [3] electrodes, the rate constant increases with the increasing concentration of the base electrolyte in a way which can be accounted for quantitatively by the Frumkin correction [2]. On the flame-annealed Au(111) and Au(110), the effect of the base electrolyte concentration is similar, though there is a difference in the rate at the same potential E relative to E_{pzc}, cf. Fig. 4. This difference is probably due to the potential dependence of the electron transfer rate related to the actual anion concentration in the solution near the electrode, vide infra.

The kinetic behaviour of the non-annealed Au(111) electrode exhibiting two well-distinguished current peaks is fairly interesting. The capacity measurements in the presence of the sulfate or peroxodisulfate anion indicated that E_{pzc} shifts negatively to a value of about −0.1 V [3]. The conclusion was then made that the reduction peak c2 observed at about the same potential is associated with the direct pathway [3]. While the correspondence between the reduction peak c1 and E_{pzc} was not obvious, it was argued that the rate of the direct pathway should have a maximum at $E \approx E_{pzc}$ due to the double layer effect [3]. On the basis of the present results, a more consistent model can be outlined, which refers to the peroxodisulfate reduction on the surface terraces and steps. There seems to be a difference in anion adsorption on these sites being linked to a difference in the local potential of zero charge. The preferential adsorption of sulfate and peroxodisulfate on steps is indicated by blocking the first stage in the oxidation of Au surface, cf. Fig. 1 and Ref. [3], which is likely to be associated with the adsorption of OH anions on step edges [20]. Towards more negative potentials, anions probably desorb easily from the terraces of Au(111), but less easily from the steps. Hence, the two reduction peaks on the non-annealed Au(111) can correspond to the electrocatalytic pathway occurring on (111) terraces (peak c1) and (111)x(111) steps (peak c2) at a rate reaching a maximum close to the local potential of zero charge. Analogously, the two reduction peaks seen on voltammograms of the Au(110) electrode (Fig. 1) can be ascribed to the electrocatalytic pathway occurring on (110) terraces and (111) × (111) steps. A similar model has been proposed for N_2O reduction on single crystal platinum electrodes to explain the observed correlation between the maximum reduction rate and the potential of the zero total charge [18]. However, this model has to be modified by considering also the direct reduction of peroxodisulfate from the solution and a strong electrostatic effect of the surface charge on its rate. Obviously, the electrocatalytic and direct pathways can overlap to some extent, because the rate of both reaches a maximum at $E \approx E_{pzc}$. In an agreement with this model,

the magnitude of the peak c2 on the flame-annealed Au(111) and Au(110) electrodes is rather negligible due to a lower density of steps on their surfaces, cf. Fig. 3.

An interesting aspect of the peroxodisulfate reduction is a hysteresis observed on voltammograms at $E < E_{pzc}$, cf. Fig. 1 and Fig. 3. The reduction current is always slightly higher on the potential sweep towards more positive potentials than on the reverse sweep. Since the hysteresis is observed mainly at far negative potentials, it should reflect a change in the rate of the direct pathway. The mechanism is likely to involve a slow potential-dependent process, which has an effect on the peroxodisulfate concentration in the solution near the electrode, and which is related to a difference in the adsorption of anions and cations on steps and/or terraces.

4.4. Evaluation of the parameters of the kinetic model

We shall assume that the rates of the direct and electrocatalytic pathways are additive, i.e. the measured rate constant k (Fig. 4) is the sum of the corresponding apparent rate constants, k_D and k_C, respectively. Since the electrocatalytic pathway prevails at $E > E_{pzc}$, the current measurements on positively charged surfaces yield the rate constant k_C directly. Analogously, the rate constant k_D can be inferred from the current measured at far negative potentials, where the direct pathway dominates. For either pathway, a simple kinetic model will be considered, whose parameters will be estimated from experimental data and used subsequently in a simulation of the kinetic behaviour in the whole potential range.

The potential dependence of the rate constant k_D can be described by the Frumkin equation [21]

$$k_D = k^0 \exp(-zF\varphi_2/RT)\exp[-\alpha_D F(E-\varphi_2)/RT] \quad (5)$$

where $z = -2$ is the anionic charge, α_D is the cathodic charge transfer coefficient and φ_2 is the potential difference across the space charge region on the solution side of the electrical double layer. An estimate of this potential can be made on the basis of the Gouy–Chapman theory,

$$\varphi_2 = (2RT/F)\sinh^{-1}\left[(\sigma + zF\Gamma_a)/\left(8\varepsilon RTc_B^0\right)^{0.5}\right] \quad (6)$$

which accounts also for the contribution of the specifically adsorbed anions [19].

Fig. 9 shows the plots of the logarithm of the rate constant k at $E < E_{pzc}$ corrected for the double-layer effect by using Eq. (5) for the Au(111) and Au(110) electrodes in 0.1 M $HClO_4$. The potential φ_2 was calculated from Eq. (6) for $z F \Gamma_a = 0$ and the surface charge density σ, which was inferred by integrating the capacity of the Au electrodes. The corrected data for both electrodes seem to fall on a single straight line with a slope corresponding to $\alpha_D = 0.28$ and $k^0 = 8 \times 10^{-2}$ cm s^{-1}. A comparable rate constant was found for Au(poly) ($k^0 \approx 5 \times 10^{-2}$ cm s^{-1}), though the charge transfer coefficient was rather low ($\alpha_D \approx 0$) [2]. The estimated kinetic parameters and the charge of the adsorbed anions $z F \Gamma_a$ (Fig. 7B) were then used in Eq. (5) and Eq. (6) to simulate the kinetics of the direct electron transfer on both negatively and positively charged electrodes, cf. the lines in Fig. 10. Obviously, a sudden drop in the rate constant due to the strong repulsion induced by the specifically adsorbed anion should occur at $E \approx E_{pzc}$.

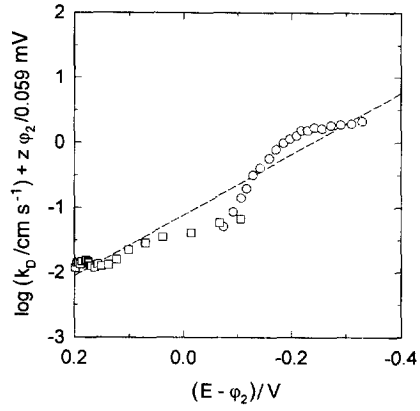

Fig. 9. Corrected rate constant vs. the corrected potential of the direct reduction pathway on the Au(111) (□) and Au(110) (○) electrodes in 0.1 M $HClO_4$ + 1 mM $Na_2S_2O_8$ evaluated for $z = -2$.

A kinetic model of the electrocatalytic pathway has been developed in the previous study [3]. The model assumes that the steady-state is established in the reaction (1a) as a result of balancing the rates of the adsorption, the desorption and the first one-electron transfer step. It has been argued [3] that the latter step determines the rate of the electrocatalytic pathway, while the second electron transfer to the highly reactive radical-anion $SO_4^{\cdot-}$ is much faster. For electrostatic reasons, the rate of the simple or a

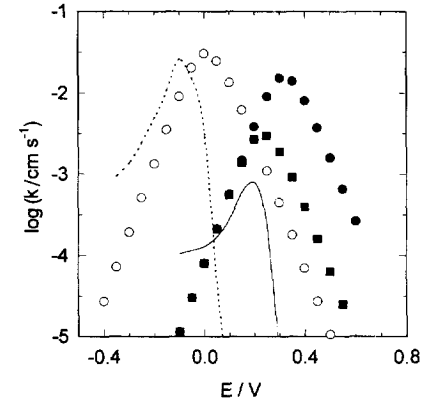

Fig. 10. Simulation of the potential dependence of the rate constants k_D and k_C of the direct (lines) and the electrocatalytic (points) reduction pathway, respectively, on the Au(110) (○, · · ·) and Au(111) (●, ————) electrodes in 0.1 M $HClO_4$ or in 0.01 M H_2SO_4 (■) for the values of the parameters given in Table 1, and the common values of the parameters $\alpha_C = \gamma' = 0.5$, $\gamma + \gamma' = 0.36$, $\beta = 0.64$, $\alpha_D = 0.28$ and $k^0 = 8 \times 10^{-2}$ cm s^{-1}.

dissociative adsorption of peroxodisulfate should decrease with the decreasing potential and, hence, the role of the adsorption as the limiting factor can be excluded. The rate constant k_C of the electrocatalytic pathway can be then expressed by the equation [3]

$$k_C = k_e^0\theta\left(c_B^0/c\right)\exp\left(-\alpha_C FE/RT\right) \quad (7)$$

where θ is the steady-state coverage of peroxodisulfate,

$$\theta/\left(1-\Sigma\theta_i\right)^3 = K_{ad}c/\left[1+K_{ed}c_B^0\right] \quad (8)$$

$K_{ad} = (k_a^0/k_d^0)\exp[(\gamma+\gamma')\ F\ E/RT]$, $K_{ed} = (k_e^0/k_d^0)\exp(-\beta\ F\ E/RT)$, k_a^0, k_d^0 and k_e^0 are the rate constant of the adsorption, desorption and electron transfer step at $E=0$, α_C is the apparent charge transfer coefficient of the electron transfer to the adsorbate, γ' or γ are the coefficients characterizing the potential dependence of the rate of the adsorption and desorption, and $\beta = \alpha_C - \gamma$. Here, the model was slightly adapted by replacing the bulk concentration c^0 by the actual concentration at the electrode c, which can be calculated from the current I, as explained above. The steady-state surface coverage θ' of the adsorbed sulfate can be described by an analogous equation which, however, introduces another set of the adsorption parameters. On the other hand, the analysis of the capacity data (Section 4.2) indicated that the ratio of the surface concentrations of sulfate and peroxodisulfate is approximately 0.5, when the solution concentrations of the anions are equal. Therefore, a simplifying assumption was used that $\theta'/c' = \theta/2c$, which made it possible to characterize the kinetic behaviour only by the parameters of Eq. (7) and Eq. (8), where the total surface coverage $\Sigma\theta_i = \theta + \theta' = \theta\,[1+(c'/2c)]$.

The values of the five parameters of the electrocatalytic pathway, i.e. α_C, β, k_e^0, k_a^0/k_d^0 and k_e^0/k_d^0 were estimated from the kinetic and adsorption data shown in Fig. 4 and Fig. 7A, respectively. As follows from Eq. (7) and Eq. (8), the slope of the log k vs. E plot is controlled by the factor $\exp(-\alpha FE/RT)$ or $\exp(\gamma' FE/RT)$ at far positive or negative potentials, respectively. When the concentration of the base electrolyte concentration is low, and the contribution from the direct electron transfer is small, the log k vs. E plots have the initial reciprocal slopes of approximately 120 mV per decade, and about the same but negative slope at far negative potentials, for both electrodes, cf. Fig. 4. These slopes correspond to $\alpha \approx 0.5$ and $\gamma' \approx 0.5$, respectively. The evaluation of other parameters is less simple, but an iterative use of Eq. (7) and Eq. (8) to fit the kinetic and adsorption data, respectively, provided eventually the values which are summarized in Table 1, and the common values $\gamma = -0.14$ and $\beta = 0.64$.

The results of the simulation are shown in Fig. 7A and Fig. 10, respectively. Obviously, with the same set of the parameters for a given electrode, the kinetic model reproduces successfully the main features of both the adsorption and kinetic behaviour. The kinetic parameters of the model characterize quantitatively two most important experimental observations. Firstly, the rate constant k_e^0 of the electron transfer to the adsorbed peroxodisulfate is indeed more than two order of magnitude higher on Au(111) than on Au(110). Secondly, in an agreement with the conclusion that the anion adsorption is controlled by the charge on the metal, the kinetic parameters of adsorption or desorption of peroxodisulfate on Au(110) and Au(111) have similar values at the same charge density σ. For example at $\sigma = 0$, which occurs at $E = E_{pzc} = -0.06$ and 0.22 V, these parameters can be calculated as $k_a^{0\prime} = k_a^0 \exp(\gamma' FE_{pzc}/RT)$ and $k_d^{0\prime} = k_d^0 \exp(-\gamma FE_{pzc}/RT)$, cf. Table 1. It is noteworthy, that the adsorption equilibrium of peroxodisulfate is not much affected by the following electron transfer at potentials $E > 0.04$ V and 0.37 V for Au(110) and Au(111), respectively, at which $K_{ed}\ c_B^0 < 0.1$ ($c_B^0 = 10$ mM), cf. Eq. (8). Hence, one of the assumptions underlying the interpretation of the results displayed in Fig. 7A as the sum of the surface concentrations of peroxodisulfate and sulfate is fulfilled in a relatively broad range of the potential E. The model has been shown already [3] to predict correctly the changes in the voltammetric peak potential E_p with the concentrations c^0 and c_B^0, which for a irreversible electrode reaction should reflect the changes in the rate constant k [3]. The theoretical values of the slopes $\partial E_p/\partial \log\ c^0 \approx -120$ mV and $\partial E_p/\partial \log\ c_B^0 \approx 120$ mV follow directly from Eq. (7), in the limit $\theta \rightarrow 1$. These are comparable with the present voltammetric data, cf. Section 3.1

Table 1
Parameters of the kinetic model of the electrocatalytic pathway in the peroxodisulfate reduction on Au(110) and Au(111)

Parameter	Au(110)	Au(111)
k_e^0, cm s^{-1}	2×10^{-3}	0.4
(k_a^0/k_d^0), mol^{-1} l	10^3	20
(k_e^0/k_d^0), mol^{-1} l	30	10^5
k_a^0, cm s^{-1}	7×10^{-2}	8×10^{-5}
$k_a^{0\prime}$, cm s^{-1}	2.6×10^{-2}	4×10^{-3}
k_d^0, cm s^{-1} mol l^{-1}	7×10^{-5}	4×10^{-6}
$k_d^{0\prime}$, cm s^{-1} mol l^{-1}	5×10^{-5}	1×10^{-5}

The increasing concentration of perchloric acid can result in two opposite kinetic effects [3]. The catalytic effect is probably associated with the proton assisting the rate-determining step in the scheme (1a). Since no difference in the reduction rate between the previously reduced and oxidized gold electrodes was observed, cf. Fig. 1, the possibility was excluded that the role of the proton is to facilitate the reduction of the surface oxides blocking the electrocatalytic pathway. Another explanation is that the electronic acceptor level on the adsorbed peroxodisulfate is lowered due to the interaction with proton, which facilitates the electron transfer. Note that the space-charge region is populated by protons compensating for the su-

perequivalent anionic adsorption. The co-adsorption of proton and sulfate on Au(111) has been indicated by the STM data [22]. On the other hand, the co-adsorption of perchlorate can lead to an inhibition of the electrocatalytic pathway, which can be accounted for by an additional contribution to the total surface coverage $\Sigma\ \theta_i$ in Eq. (8) [3]. While the present study has not provided convincing evidence for such an effect of perchlorate, the electrocatalytic pathway is clearly inhibited in the presence of sulfate, cf. the dotted line in Fig. 4. The kinetic behaviour of the system, in which the base electrolyte is sulfuric acid, was simulated by using Eq. (7) and Eq. (8) for the values of the parameters for Au(111) given above and the total surface coverage $\Sigma\ \theta_i = \theta + \theta' = \theta\ \{1 + [(c' + c_B^0)/2c]\}$, cf. Fig. 10. This simulation confirms that the decrease in the reduction rate observed at more positive potentials originates from the enhanced adsorption of sulfate.

5. Conclusions

The vast majority of Au atoms on Au(110) and Au(111) surfaces is found on the unreconstructed terraces of the expected rectangular and trigonal symmetry, respectively, the step density being comparable for both surfaces, yet lower than on a non-annealed surface.

Strong adsorption of peroxodisulfate and/or sulfate on both surfaces is observed, which has the superequivalent character, and which is controlled mainly by the charge on the metal. An interesting aspect of the superequivalent adsorption is that the anions, including peroxodisulfate, are depleted from the space charge region even on the positively charged surface. As a result, the rate of the reduction of solution species (the direct pathway) becomes negligible, and the reaction proceeds mainly via the electron transfer to the adsorbed peroxodisulfate (the electrocatalytic pathway). The surface structure and symmetry of Au(111) surface allow for a more effective overlap of the electronic wave functions of the metal and the adsorbed peroxodisulfate, which results in a two order of magnitude faster electron transfer than on Au(110).

On negatively charged surfaces, the rate of the electrocatalytic pathway is limited by the decreasing surface concentration of peroxodisulfate, while the rate of the direct pathway can be measured. Its correction for the double-layer effect reveals that the true kinetic parameters of the direct pathway have essentially the same values for both electrodes.

A comparison of the kinetic behaviour of the flame-annealed and non-annealed Au(111) electrodes throws some light on the role of steps on the metal surface. A difference in the local potential of zero charge between surface steps and terraces, can be responsible for a difference in the rates of both the direct and electrocatalytic pathways, the latter probably being linked to a difference in the anion adsorption on these sites. The corresponding maximum of the reduction current can serve as an indication of the position of the potential of zero charge.

Acknowledgements

Z.S. acknowledges gratefully financial support from the Max-Planck-Gesellschaft. This work was supported in part by the Grant Agency of the Czech Republic, grant. no. 203/96/1090.

References

[1] R. Parsons, Surf. Sci. 2 (1964) 418.
[2] Z. Samec, K. Doblhofer, J. Electroanal. Chem. 367 (1994) 141.
[3] Z. Samec, A.M. Bittner, K. Doblhofer, J. Electroanal. Chem. 409 (1996) 165.
[4] A.N. Frumkin, N.V. Nikolaeva-Fedorovich, N.P. Berezina, Kh.E. Keis, J. Electroanal. Chem. 58 (1975) 189.
[5] A.J. Bard, L.R. Faulkner, Electrochemical Methods, Wiley, New York, 1980.
[6] J. Desilvestro, M.J. Weaver, J. Electroanal. Chem. 234 (1987) 237.
[7] Z. Shi, J. Lipkowski, M. Gamboa, P. Zelenay, A. Wieckowski, J. Electroanal. Chem. 366 (1994) 317.
[8] B. Timmer, M. Sluyters-Rehbach, J.H. Sluyters, J. Electroanal. Chem. 14 (1967) 169.
[9] M. Sluyters-Rehbach, J.H. Sluyters, in: E. Yeager, J.O'M. Bockris, B.E. Conway, S. Sarangapani (Eds.), Comprehensive Treatise of Electrochemistry, Vol. 9, Plenum, New York, 1984, p. 177.
[10] A.M. Bittner, J. Wintterlin, G. Ertl, J. Electroanal. Chem. 388 (1995) 225.
[11] O.M. Magnussen, J. Wiechers, R.J. Behm, Surf. Sci. 289 (1993) 139.
[12] W. Haiss, D. Lackey, J.K. Sass, K.H. Besocke, J. Chem. Phys. 95 (1991) 2193.
[13] O.M. Magnussen, J. Hageböck, J. Hotlos, R.J. Behm, Faraday Discuss. 94 (1992) 329.
[14] C.M. Vitus, A.J. Davenport, J. Electrochem. Soc. 141 (1994) 1291.
[15] X. Gao, M.J. Weaver, J. Electroanal. Chem. 367 (1994) 259.
[16] R. Parsons, J. Electroanal. Chem. 8 (1964) 93.
[17] A. Hamelin, T. Vitanov, E. Sevastyanov, A. Popov, J. Electroanal. Chem. 145 (1983) 225.
[18] G.A. Attard, A. Ahmadi, J. Electroanal. Chem. 389 (1995) 175.
[19] D.M. Mohilner, in: A.J. Bard (Ed.), Electroanalytical Chemistry, Dekker, New York, 1966, p. 241.
[20] S. Štrbac, R.R. Adžić, A. Hamelin, J. Electroanal. Chem. 249 (1988) 291.
[21] A.N. Frumkin, G.M. Florianovich, Dokl. Akad. Nauk SSSR 80 (1951) 907.
[22] G.J. Edens, X. Gao, M.J. Weaver, J. Electroanal. Chem. 375 (1994) 357.